

## Encapsulation of beetroot extract (*Beta vulgaris* L.) obtained by internal and external ionic gelation: a comparative study

Joana de Barros ALEXANDRE<sup>1</sup> , Tiago Linhares Cruz Tabosa BARROSO<sup>2</sup> , Luana Carvalho da SILVA<sup>3</sup> ,  
Rachel Menezes CASTELO<sup>1</sup> , Gabrielle Albuquerque FREIRE<sup>1</sup> , Amanda Batista NASCIMENTO<sup>1</sup> ,  
Huai Nan CHENG<sup>4</sup> , Atanu BISWAS<sup>5</sup> , Laura Maria BRUNO<sup>6</sup> , Roselayne Ferro FURTADO<sup>6\*</sup> 

### Abstract

Natural pigments, like betalains found in beets, are sensitive to environmental conditions, which may impact their reactivity and shelf-life. Microencapsulation is an attractive alternative for delivering these compounds, offering protection through polymeric microcapsules. The aim of this study was to compare two ionic gelation methodologies, external (EG) and internal gelation (IG), in the microencapsulation of beet aqueous extract. Particles were obtained by mixing sodium alginate with the aqueous extract of beetroot and crosslinking with calcium chloride solution using the extrusion method. Encapsulation characteristics and physical, morphological features were evaluated. The particles showed 10.72 and 89.90% encapsulation efficiency for EG and IG, respectively. Loading capacity was 18.90% for EG and 25.60% for IG. Those IG particles showed superior water absorption capacity during rehydration. Texture analysis indicated that EG particles showed greater hardness. Release kinetics indicated that EG particles followed the Korsmeyer-Peppas model, while IG particles followed the Higuchi model. Thus, the appropriate encapsulation technique should be selected depending on the food matrix to be used and the specific objective of delivering the active encapsulated molecules.

**Keywords:** alginate; encapsulation; controlled release; food additive.

**Practical application:** The mechanism of ionic gelation influences the final characteristics of the particles.

## 1 INTRODUCTION

Beetroot (*Beta vulgaris* L.) is rich in betalain compounds, water-soluble pigments containing nitrogen, which are characterized by their high antioxidant activity, with potential applications in the food, cosmetic, and pharmaceutical industries (Rodríguez-Félix et al., 2022; Yang et al., 2021). Betalain derivatives can be classified as betacyanins (red-violet color) and betaxanthins (yellow-orange color) (Celli & Brooks, 2017; Luiza Koop et al., 2022). However, natural food dyes and pigments, such as betalains, have poor thermal stability and may be unstable in the presence of oxygen and light (Li et al., 2022). In addition, beetroot betalains are marred by an earthy taste (Luiza Koop et al., 2022). Encapsulation technology is a well-known method to protect bioactive compounds from adverse conditions and mask unpleasant flavors/odors by forming a protective barrier with the encapsulated compound, thereby extending the shelf-life of the substances and providing controlled release under specific conditions (Alexandre et al., 2019; Barroso et al., 2021).

Among the encapsulation techniques, ionic gelation is used to obtain particles from nano to macro sizes and offers advantages over many other methods due to its simplicity,

cost-effectiveness, and independence from high temperatures or organic solvents (Kurtulbaş et al., 2022; Otálora et al., 2018). In gastronomy, the ionic gelation technique is commonly known as basic spherification (external ionic gelling) and reverse spherification (internal ionic gelation), used for preparing caviar, ravioli, pasta, teas, and other beverages.

This study compares beetroot particles obtained by external ionic gelation (EG) and internal gelation (IG) techniques based on their characteristics. EG occurs from the interaction of the dripped alginate polymeric solution into an ionic solution, such as calcium chloride, under constant agitation. The compound to be encapsulated is mixed with the polymeric solution, and spherical gel structures form as the drops reach the ionic solution (Da Silveira Cáceres de Menezes et al., 2015; Kurozawa & Hubinger, 2017). On the other hand, IG produces particles from an insoluble calcium salt, for example, calcium carbonate, dispersed in a polymeric solution containing the active agent. The solution is dripped into an acidified oil medium where  $\text{Ca}^{2+}$  ions are released, leading to alginate crosslinking (Kurozawa & Hubinger, 2017). Studies have reported that the encapsulation of hydrophilic compounds by IG can be a useful methodology

Received 21 Nov., 2023.

Accepted 12 Dec., 2023.

<sup>1</sup>Universidade Federal do Ceará, Postgraduate Program in Natural Sciences, Fortaleza, Ceará, Brazil.

<sup>2</sup>Universidade Estadual de Campinas, School of Food Engineering, Campinas, São Paulo, Brazil.

<sup>3</sup>Universidade Federal do Ceará, Science and Technology Center, Fortaleza, Ceará, Brazil.

<sup>4</sup>Southern Regional Research Center, USDA Agricultural Research Service, New Orleans, Louisiana, United States of America.

<sup>5</sup>National Center for Agricultural Utilization Research, USDA Agricultural Research Service, Peoria, Illinois, United States of America.

<sup>6</sup>Brazilian Agricultural Research Corporation, Embrapa Tropical Agroindustry, Fortaleza, Ceará, Brazil.

\*Corresponding author: [roselayne.furtado@embrapa.br](mailto:roselayne.furtado@embrapa.br)

to avoid diffusion into the crosslinking solution, enhancing encapsulation efficiency and promoting homogeneous gel formation (Belščak-Cvitanović et al., 2016; Kurozawa & Hubinger, 2017; Wang et al., 2023).

In this work, sodium alginate was chosen as the polymer to encapsulate betalain. Alginate is a polysaccharide normally extracted from the cell wall of brown algae and widely used in ionic gelling techniques due to its biodegradability, filmogenic properties, non-toxicity, and lack of interaction with the active principle. In the presence of bivalent cations like  $\text{Ca}^{2+}$ , alginate undergoes a transition from solution to gel (Dodero et al., 2019; Kurozawa & Hubinger, 2017; Kurtulbaş et al., 2022; Noor et al., 2022).

Thus, the aim of this study was to encapsulate betalains in beetroots extract using the ionic gelation technique. The performance of particles formed by both EG and IG was evaluated and compared in terms of encapsulation efficiency, morphology, mechanical properties, pH resistance, and release kinetics.

## 2 MATERIALS AND METHODS

### 2.1 Materials

Beetroot and canola oil were purchased at a local market in Fortaleza. The chemical reagents, including alginate, acetic acid, citric acid, sodium citrate, calcium chloride, and calcium carbonate, were purchased from *Dinâmica Química Contemporânea Ltda.* (São Paulo, Brazil).

### 2.2 Extraction of compounds from beetroot

The beetroots were sanitized, cut with peels, and added to water in a ratio of 1:2 (m/v). Then, they were crushed in a blender, and the mixture was adjusted to pH 5.5 with 0.2 M citric acid. Afterwards, the solution underwent ultrasound treatment with a 22-mm diameter probe (Hielscher Ultrasonics HmnH, model UP 400S, 24 kHz) for 20 minutes. Finally, the extract was frozen in an ultrafreezer (Sanyo VIP, Temperature Freezer Model MDF-U33V) at  $-85^{\circ}\text{C}$  for freeze-drying (CHRIST, model 1-8 LSC basic). The resultant dry mass was ground in a knife mill and stored in polypropylene bags away from light.

### 2.3 Formation of particles by external and internal gelation

The particles were obtained via EG, according to Castelo et al. (2020), with adaptations. For encapsulation, 10 mL of alginate solution 2% (m/v) was mixed with 3.3 mL of aqueous beet extract (1:20) (m/v) to obtain a final concentration of 1.5% (v/v). The solution was inserted into the encapsulator (Büchi, model B-395, Essen, Germany) with a 120  $\mu\text{m}$  drip nozzle, flow rate of 5 mL/min, and frequency of 1,800 Hz. The solution was dropped into a calcium chloride solution of 2% (m/v), followed by washing with distilled water to remove excess salt.

The methodology to obtain particles by IG was adapted from Basu et al. (2018). For encapsulation, 13 mL of alginate solution 2% (m/v) was mixed with 3.3 mL of aqueous beet extract (1:20) (m/v) and 1 mL of calcium carbonate 3.6% (m/v)

to obtain a final concentration of 1.5% (v/v). The solution was inserted into the encapsulator (Büchi, model B-395) with a 120  $\mu\text{m}$  drip nozzle, a flow rate of 5 mL/min, and a frequency of 1,800 Hz. The solution was dropped into 50 mL of canola oil with 80  $\mu\text{L}$  of glacial acetic acid. Then, the particles were washed with distilled water to remove excess oil.

## 2.4 Evaluation of encapsulation of beetroot extract

### 2.4.1 Encapsulation efficiency

Encapsulation efficiency (EE) was determined by weighing 0.5 g of particles and immersing them in 25 mL of sodium citrate solution 3% (m/v), according to Silva et al. (2022), with adaptations. The samples were stirred for 10 minutes on a magnetic stirrer and then assayed using a spectrophotometer (Cary 50 Conc, California). The values were expressed as total betalain content from the sum of the concentrations of betacyanins (535 nm) and betaxanthins (490 nm). For quantification, standard curves were established for betacyanins ( $y = 0.0005x + 0.0153$ ;  $R^2 = 0.99$ ) and betaxanthin ( $y = 0.0003 + 0.0212x$ ;  $R^2 = 0.99$ ) of the beetroot extract (Equation 1).

$$EE = \left( \frac{Tb}{Ti} \right) \times 100 \quad (1)$$

Where:

*Tb*: the total betalain content, representing the amount of betalain recovered after particle rupture;

*Ti*: the initial content of betalains used in encapsulation.

### 2.4.2 Loading capacity

Loading capacity (LC) can be defined as the amount of active ingredient loaded per unit mass of carrier particle. LC was determined by weighing 0.5 g of particles, and was calculated from Equation 2.

$$LC = \left( \frac{mb}{mt} \right) \times 100 \quad (2)$$

where:

*mb*: the mass of the active ingredient (betalain);

*mt*: the total mass of the particle (active ingredient + carrier material).

## 2.5 Morphological and mechanical characterization of particles

### 2.5.1 Optical morphology, particle size and sphericity

Particle size was determined through images obtained with an optical microscope (Zeiss, model Axio Imager A2). Micrographs were captured from random samples of five particles. Measurements of transverse and longitudinal particle

diameters were performed and the average size was calculated using the Ferret diameter method (Zanetti et al., 2002), according to Equation 3.

$$TM = \frac{d+D}{2} \quad (3)$$

Where:

TM: the average size;

d: the smallest diameter of an inscribed circle;

D: the largest diameter of the circumscribed circle, both concerning the largest cross-section of the particle.

The degree of sphericity of the particles was determined using the Riley method (Riley, 1941), as indicated in Equation 4.

$$\Phi_0 = \sqrt{\frac{d}{D}} \quad (4)$$

where:

$\Phi_0$ : the sphericity;

d: the smallest diameter of an inscribed circle;

D: the largest diameter of the circumscribed circle, both in relation to the largest cross-section of the particle.

### 2.5.2 Determination of mechanical properties

Texture analysis of particles was performed as described by Deladino et al. (2008), with adaptations. Seven grams of particles were weighed and placed in a petri dish with a diameter of 50 mm to fill the entire surface, forming a single layer. A texturometer (Stable Micro Systems Ltd., model TA-TX2i) equipped with a 30 kg load cell was used. Compression was performed using a probe of 0.5 mm diameter at a test speed of 1 mm/sec and 2 g trigger. The results were expressed in Newtons (N).

### 2.5.3 Swelling analysis

The swelling degree (SD) of the particles after drying was determined according to the methodology proposed by Xu et al. (2003). The total mass of the initial sample ( $M_i$ ) was quantified in a Gooch filter, which was then immersed in distilled water for 24 h. Excess water was removed, and the final wet mass ( $M_f$ ) was determined. The swelling degree was calculated based on the initial mass of the sample, according to Equation 5.

$$SD = \frac{M_f - M_i}{M_f} \quad (5)$$

where:

SD: the swelling degree;

$M_f$ : the final wet mass;

$M_i$ : the initial total mass.

### 2.5.4 Resistance to different pH values

The resistance of the particles was determined at pH values of 2, 3, 4, 5, 6, and 7. Each sample was immersed in 25 mL of water, and the pH was adjusted with 0.1 M hydrochloric acid or 0.1 M sodium hydroxide. Then, readings were taken using a spectrophotometer (Cary 50 Conc, California) at wavelengths of 490 nm for betaxanthins and 535 nm for betacyanins.

### 2.6 Release study and kinetic evaluation

The release study was performed by varying time intervals from 0 to 120 minutes. A total of 0.5 g of particles was added to 25 mL of water. Samples aliquots of the solution were taken at different times and analyzed using a spectrophotometer (Cary 50 Conc), at wavelengths of 490 nm for betaxanthins and 535 nm for betacyanins.

To assess the release mechanism, the data were fitted to mathematical models that describe zero-order, first-order, Higuchi, and Korsmeyer-Peppas kinetics (Equations 6–9), as defined by Silva et al. (2022):

$$\text{Zero-order: } Q = Q_0 - K_0 t \quad (6)$$

$$\text{First-order: } \ln Q = \ln Q_0 - K_1 t \quad (7)$$

$$\text{Higuchi: } Q = K_H t^{1/2} \quad (8)$$

$$\text{Korsmeyer-Peppas: } Q = K_{KP} t^n \quad (9)$$

where:

Q: the amount of active ingredient released at time t;

$Q_0$ : the initial amount of active ingredient in the solution;

n: the diffusion exponent indicative of the transport mechanism of the active ingredient;

$K_0$ ,  $K_1$ ,  $K_H$ , and  $K_{KP}$ : release rate constants for the respective models.

### 2.7 Statistical analysis

Analysis of variance (ANOVA) with repeated measures was used to evaluate statistically significant variables and their interactions. Significant differences between samples were determined using Tukey's test ( $p \leq 0.05$ ). Statistica® software was used for the statistical analysis (version 10.0, StatSoft Inc.).

### 3 RESULTS AND DISCUSSION

#### 3.1 Evaluation of beetroot extract encapsulation

##### 3.1.1 Encapsulation efficiency and Loading capacity

EE and LC are two essential parameters for the evaluation of the encapsulation process. High EE values indicate a significant amount of the active compound in the particle. EE values varied between 10.72 and 89.90% for the EG and IG techniques, respectively. It was possible to observe that the betalain content of EG particles was quickly diffused into the crosslinking solution due to concentration differences between the aqueous solution and capsules. However, for lipophilic compounds, EG demonstrated better encapsulation efficiency than IG, as it reduces interactions with the environment (Somacal et al., 2022). In addition, the particles produced by EG have a porous gel structure, which allows the quick and easy diffusion of water and other fluids both inside and outside the matrix particle (da Silva Carvalho et al., 2019; Naranjo-Durán et al., 2021; Somacal et al., 2022). Our results suggest that IG could serve as an alternative for encapsulating hydrophilic compounds to minimize or prevent their diffusion toward the crosslinking solution, since the encapsulation process occurs in the oil phase, resulting in higher EE in these cases (Li et al., 2023).

Particles obtained by EG and IG presented LC of 18.90 and 25.60%, respectively. The literature reports that > 50% loads have disadvantages in encapsulation, since it reduces the protection of the active material and facilitates its release into the media (Shaddel et al., 2018). Consequently, lower LC values offer better protection and are related to particle morphology and size (Calderón-Oliver et al., 2017).

#### 3.2 Morphological and mechanical characterization of particles

##### 3.2.1 Optical morphology

The morphological characteristics of EG and IG particles were evaluated regarding their morphology both before and after the drying and rehydration processes (Figure 1). Particles from both encapsulation methods (Figures 1A and 1B) exhibited smooth surfaces with no apparent cracks. Following drying by lyophilization and subsequent rehydration in distilled water for 24 hours (Figures 1C and 1D), morphological analysis was carried out. The EG particle obtained had a more significant change on its surface, with a more wrinkled appearance. This change may be attributed to a more porous matrix, facilitating greater diffusion from the material to the external environment (Yousefi et al., 2020), causing particle deformity.

In contrast, the IG particle, with its more compact matrix, allowed only the slightest changes in the spherical appearance. Similar results were found by Lupo et al. (2015), where particles produced by EG exhibited greater porosity in their microstructure compared to those obtained by IG, which displayed a more compact structure. Da Silva Carvalho et al. (2019) observed a macroporous structure in alginate capsules produced using the EG technique, allowing extensive interaction of the active

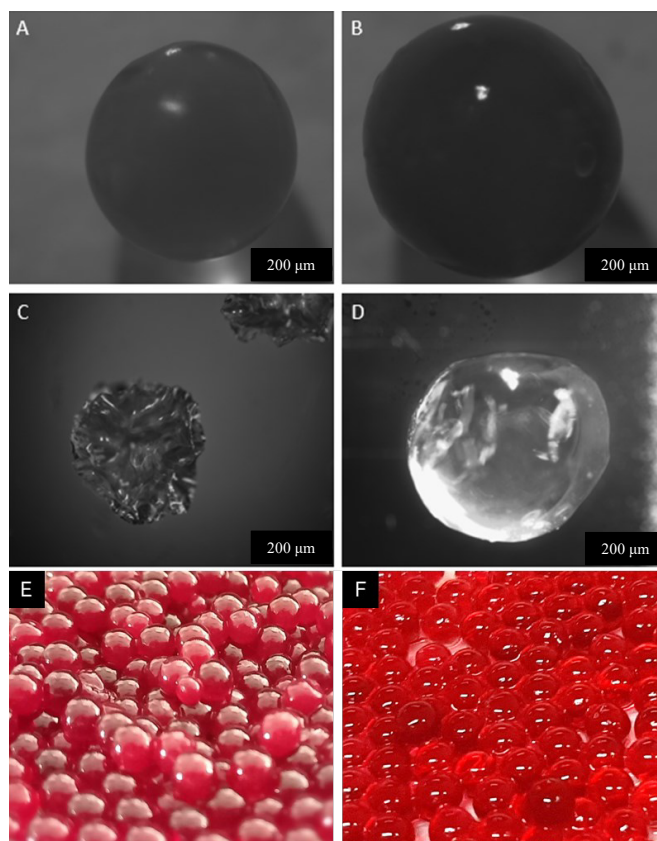


**Figure 1.** Optical micrographs and particles of betalain extract. (A) EG particles, (B) IG particles, (C) rehydrated EG particles, (D) rehydrated IG particles, (E) visual aspect of EG particles, and (F) visual aspect of IG particles.

agent with the external environment, such as oxygen, potentially leading to the degradation of active compounds. Therefore, the selection of the encapsulation method and subsequent drying are crucial for enabling longer storage time and maintenance of the biological properties of the encapsulated material (Zhang et al., 2020). Visually, it is noticeable that the IG particle (Figure 1F) displayed a brighter surface than the EG particle (Figure 1E).

##### 3.2.2 Particle size and sphericity

The particles obtained had an average diameter (AD) of  $750.17 \pm 23.98 \mu\text{m}$  for EG and  $2,680.23 \pm 29.73 \mu\text{m}$  for IG. Several factors may influence the size and shape of alginate particles, e.g., the surface tension and viscosity of the alginate solution and the concentration of salt used in the reticulation of the encapsulating matrix (Kurtulbaş et al., 2022). Sphericity values were  $0.95 \pm 0.01$  for EG and  $0.98 \pm 0.01$  for IG; both are close to one (1), indicating that the resulting particles are spherical. Sphericity values relative to those found in this work were also reported by Castelo et al. (2020), who used the same frequency of 1,800 Hz to form alginate particles to encapsulate *pequi* oil. The desirable sphericity of the particles suggests that both the surface tension of the alginate solution and the operational parameters of encapsulation were optimized to yield homogenous particles (Labus et al., 2018).

### 3.2.3 Swelling analysis

After freeze-drying, the rehydrated particles (Figure 2) showed swelling values between 82 and 85% for EG and from 92 to 97% for IG, attesting that the particles obtained by IG exhibited greater rehydration capacity than those obtained by EG. The IG particles exhibited rapid rehydration within the first few hours, followed by equilibrium in the swelling rate.

The swelling capacity is related to the presence of  $\text{Ca}^{2+}$  ions during the crosslinking step, which in the case of the EG particles happens in the external structure. The particles appeared hard, and presented greater hardness in texture analysis. The  $\text{Ca}^{2+}$  content and the force of attraction with alginate promoted reduced swelling (Günter et al., 2020; Li et al., 2019). Conversely,

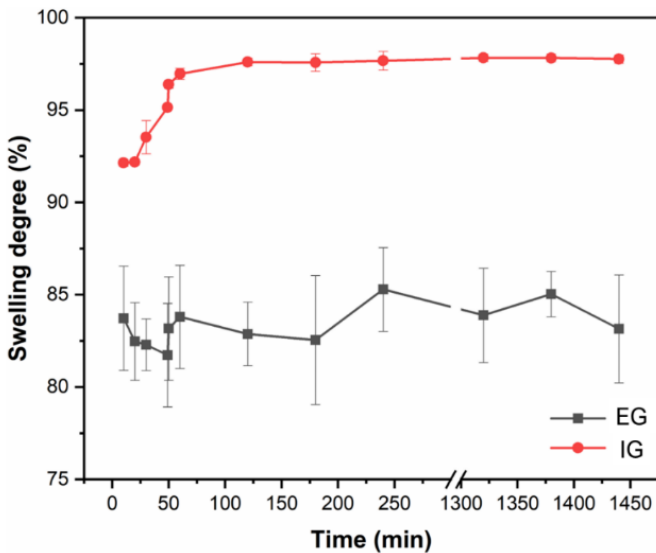


**Figure 2.** Swelling analysis of beet extract particles from EG and IG for 1,450 minutes.

IG particles (Figures 1C and 1D) were obtained in the sample's presence of insoluble calcium salt before gelation in acidified canola oil (Zhang et al., 2023). This mechanism favored obtaining particles with lower hardness and greater capacity to absorb water.

### 3.2.4 Determination of mechanical properties

The evaluation of particle hardness resulted in  $3.83 \pm 0.54$  N and  $1.12 \pm 0.10$  N for EG and IG, respectively. These results indicate that EG particles were significantly harder than IG ones ( $p < 0.05$ ). Similar findings were reported by Rajmohan and Bellmer (2019) in the characterization of spirulina particles formed by ionic gelation, and by Lupo et al. (2015) in comparing ionic gelling techniques in cocoa extract encapsulation, corroborating our findings in which the particles obtained by EG showed greater hardness than those obtained by IG. This behavior is related to the crosslinking of particles in the presence of  $\text{Ca}^{2+}$  ions. In EG, ions diffuse from an external source into the polymeric solution, whereas for IG, an insoluble calcium salt is added to the polymeric matrix containing the compound to be encapsulated, releasing ions in an acidic medium (Kouamé et al., 2021; Lupo et al., 2015).

### 3.2.5 Resistance of particles to different pH values.

The particles obtained were also evaluated at different pH values (2, 3, 4, 5, 6, and 7) (Figure 3). This analysis is especially important for potential applications of these particles since betalain stability may be pH-dependent.

In general, betalain stability was better preserved in the EG particles (Figure 3A). The highest betalain release occurred at pH 4–5, significantly different from other pH values. This can be rationalized by a disorder in the calcium-alginate structure when the particles are above the  $pK_a$  values of manuronic acid ( $pK_a = 3.38$ ) and glucuronic acid ( $pK_a = 3.65$ )

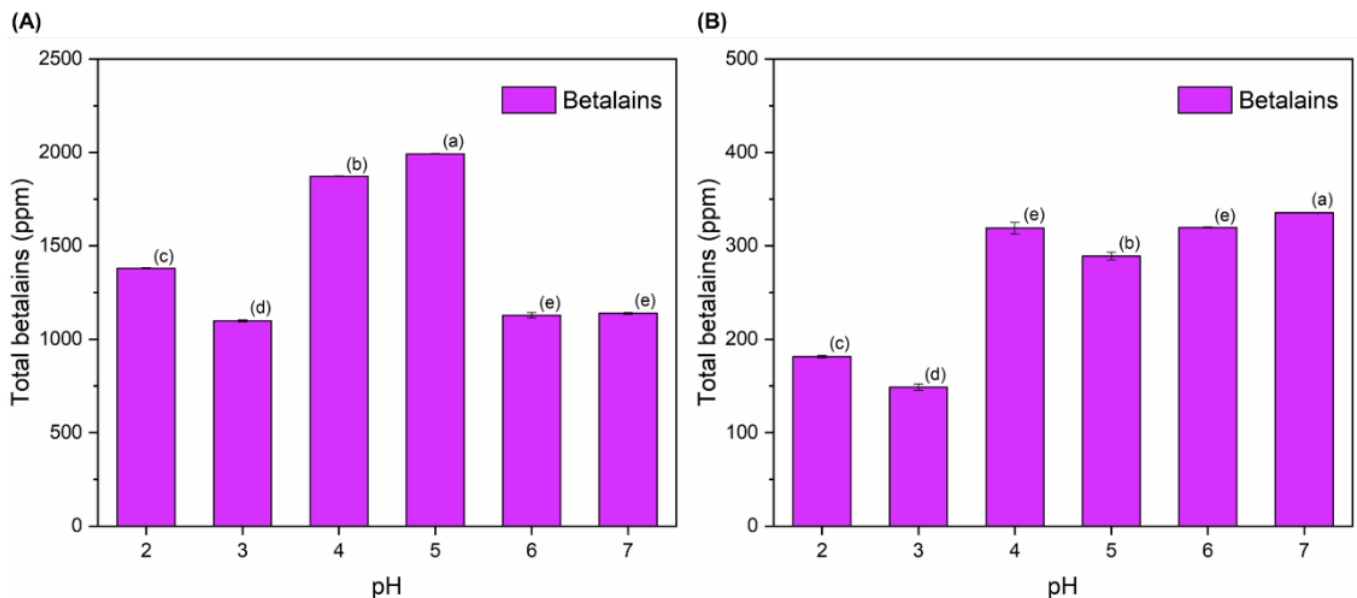


**Figure 3.** Release of betalain from particles subjected to a pH range of 2 to 7. (A) External ionic gelation and (B) Internal ionic gelation.

(Wongverawattanukul et al., 2022), the building blocks of alginate (Dalponte Dallabona et al., 2020).

At pH values below  $pK_a$ , the carboxylic groups of alginate are in COOH form, increasing hydrogen-bonding strength. The opposite effect occurs at higher pH when the carboxylic groups are in COO<sup>-</sup> form. This negative charge causes repulsion of the alginate polymer chain, leading to polymer swelling and facilitating the release of the encapsulated compound (Camacho et al., 2019). Thus, IG particles had a higher release of betalains at pH 7, due to the conditions under which they are formed. Alginate matrices have been widely used in encapsulation for release in the lower gastrointestinal tract due to their pH-dependent release (Waqas et al., 2022).

### 3.6 Release study over time and kinetic evaluation

#### 3.6.1 Study of Release

The release profile of the encapsulated active material is essential to understand the release mechanism (Silva et al., 2022). In the release of betalain particles in water (Figure 4), EG particles showed a rapid release of the active compound up to 120 min (“burst” effect), with a more pronounced effect between 20 and 40 min. Still, the release effect was maintained until the maximum time was analyzed (120 min). On the other hand, the IG particles obtained their “burst” effect up to 40 min, reaching maximum release with no further changes until 120 min. Therefore, for the subsequent study of release kinetics, values up to 120 min for EG particles and up to 40 min for IG particles will be considered. EG particles reached a final release of 60% at 120 min, while IG particles reached a maximum final release of 100% in the same time frame (Figure 4).

Studies reported by Lin et al. (2021) found that particles prepared via EG had stronger crosslinking between Ca<sup>2+</sup> ions and alginate molecules compared to particles prepared through IG. This phenomenon also explains the lower release of betalain

observed in EG particles due to the matrix’s increased rigidity stemming from enhanced interaction with alginate. Lupo et al. (2015) confirmed the formation of a significantly rigid layer on the surface of the particles prepared using EG, leading to greater external hardness, justifying its lower release rate. According to those authors, during EG, an outer layer of gel was formed, delaying the diffusion of calcium ions into the interior of the macroparticles; thus creating a heterogeneous matrix with a poorly crosslinked core due to the lack of calcium ions.

#### 3.6.2 Kinetic study

The results obtained up to 120 min and 40 min for EG and IG particles were analyzed using mathematical models to simulate the release mechanism of the active material from the particles. The values of the kinetic parameters used for the applied models are shown in Table 1.

The zero-order and first-order models, applied to both EG and IG particles, yielded R<sup>2</sup> values significantly below the ideal (0.99). This suggests that these models, which predict a simple linear release, were not adequate. Instead, the Higuchi and Korsmeyer-Peppas models were preferred, as shown in Table 1. For EG particles, the Korsmeyer-Peppas model obtained a high R<sup>2</sup> value (0.95), indicating its adequacy in describing betalain release from these particles. For the IG particles, the Higuchi model presented the highest R<sup>2</sup> value (0.95); a similar result was also reported by Budinčić et al. (2021) and Silva et al. (2022). The Higuchi model is generally used to study the release of water-soluble and poorly soluble materials incorporated in semisolid and/or solid matrices (Costa, 2002). The Korsmeyer-Peppas model is generally used to analyze polymeric systems with unknown release mechanisms or when more than one type of release may be involved (Costa, 2002).

According to the literature, the value of  $n = 0.43$  corresponds to the release of the active substance by diffusion according to Fick’s law, while values below 0.43 indicate pseudo-Fickian diffusion (Ferreira et al., 2019). Intermediate  $n$

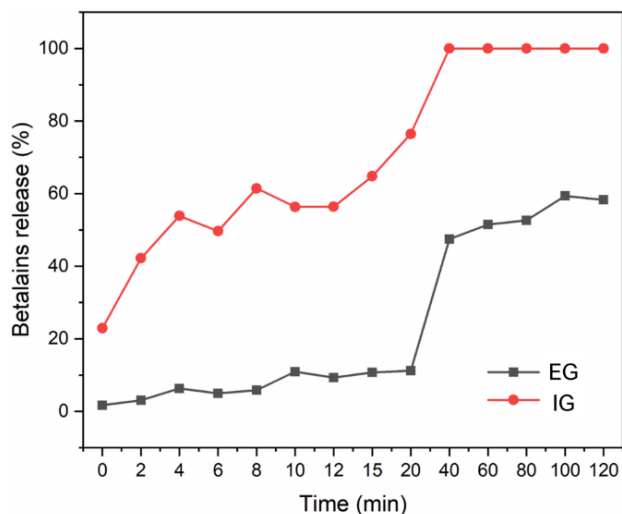


**Figure 4.** Release of beet extract particles obtained by EG and IG particles in distilled water (pH 7) over time.

**Table 1.** Kinetic parameters for the release of external gelation and internal gelation particles using mathematical models of zero-order, first-order, Higuchi, and Korsmeyer-Peppas.  $K$  is the release constant, R<sup>2</sup> is the correlation coefficient, and  $n$  is the diffusion exponent.

Mathematical model	EG	IG
Zero-order		
$K_0$	0.56	1.64
R <sup>2</sup>	0.88	0.87
First-order		
$K_1$	0.03	0.03
R <sup>2</sup>	0.76	0.67
Higuchi		
$K_H$	26.63	11.45
R <sup>2</sup>	0.92	0.95
Korsmeyer-Peppas		
$K_{kp}$	1.56	28.02
R <sup>2</sup>	0.95	0.85
$n$	0.79	0.34

values (0.43–0.89) indicate non-Fick diffusion (Zhu et al., 2022). In this work, diffusion exponent  $n$  ranged from 0.79 to 0.33 for EG and IG particles. Thus, betalain release in EG particles adhered to the Non-Fickian diffusion mechanism, signifying the coexistence of Fickian diffusion and matrix dissolution. Similar results were obtained by Wang et al. (2020), who obtained diffusion coefficient values between 0.47 and 0.52 following the non-Fickian diffusion mechanism, which is, as reported by the authors, the coexistence of Fickian diffusion and corrosion diffusion. For IG particles,  $n$  values below 0.43 indicate pseudo-Fickian diffusion, akin to a Fickian process. Lupo et al. (2015) also obtained  $n$ -values lower than 0.43, which may be related to the presence of calcium in the release medium, which may persist in alginate crosslinking, delaying betalain release. For EG particles, according to Lupo et al. (2015), the calcium concentration is more located in the outer region of the particle, which requires more than one process, in addition to the diffusion process, for the release of betalain to occur.

#### 4 CONCLUSION

The selection of the encapsulation method is of great importance and depends on the encapsulated active agent and the food matrix. In this study, a significantly higher amount of beet extract was encapsulated via internal ionic gelation, which can be an essential differential for the choice of this technique. The type of ionic gelling mechanism directly influences the technological characteristics of the particles. More significant, brighter, more elastic particles with greater water absorption capacity were found with internal ionic gelation. On the other hand, particles obtained by external ionic gelation showed a more resistant wall with a lower betalain release rate over 120 minutes. The encapsulating matrix's structure also influenced the particles' release profile in relation to pH, with a greater tendency for release in a neutral medium for particles from internal ionic gelation and in an acid medium for particles obtained by external ionic gelation. Finally, both EG and IG processes are promising for encapsulation and can mitigate the chances of chemical compound degradation.

#### ACKNOWLEDGMENTS

This work was supported by the Brazilian National Council for Scientific and Technological Development (Conselho Nacional de Desenvolvimento Científico e Tecnológico – CNPq, Brazil) (productivity grants 408599/2018-9) and Coordenação de Aperfeiçoamento de Pessoal de Nível Superior (CAPES, Brazil) (Finance code 001). The authors would like to thank CAPES and FUNCAP for granting the scholarships and the Brazilian Agricultural Research Corporation (Empresa Brasileira de Pesquisa Agropecuária – EMBRAPA) for the infrastructure provided. This work was also partly supported by the U.S. Department of Agriculture, Agricultural Research Service. Mention of trade names or commercial products is solely for the purpose of providing specific information and does not imply recommendation or endorsement by USDA. USDA is an equal opportunity provider and employer.

#### REFERENCES

- Alexandre, J. B., Barroso, T. L. C. T., Oliveira, M. A., Mendes, F. R. S., Costa, J. M. C., Moreira, R. A., & Furtado, R. F. (2019). Cross-linked coacervates of cashew gum and gelatin in the encapsulation of pequi oil. *Ciência Rural*, 49(12), 1-12. <https://doi.org/10.1590/0103-8478cr20190079>
- Barroso, T. L. C. T., Alexandre, J. de B., Silva, L. C. da, Castelo, R. M., Ribeiro, L. B., Furtado, R. F., & Zambelli, R. A. (2021). Tecnologia de encapsulamento na área de alimentos: Uma revisão. *Research, Society and Development*, 10, e6210716240.
- Basu, S., Banerjee, D., Chowdhury, R., & Bhattacharya, P. (2018). Controlled release of microencapsulated probiotics in food matrix. *Journal of Food Engineering*, 238, 61-69. <https://doi.org/10.1016/j.jfoodeng.2018.06.005>
- Belščak-Cvitanović, A., Bušić, A., Barišić, L., Vrsaljko, D., Karlović, S., Špoljarić, I., Vojvodić, A., Mršić, G., & Komes, D. (2016). Emulsion templated microencapsulation of dandelion (*Taraxacum officinale* L.) polyphenols and  $\beta$ -carotene by ionotropic gelation of alginate and pectin. *Food Hydrocolloids*, 57, 139-152. <https://doi.org/10.1016/j.foodhyd.2016.01.020>
- Budinčić, J. M., Petrović, L., Đekić, L., Fraj, J., Bučko, S., Katona, J., & Spasojević, L. (2021). Study of vitamin E microencapsulation and controlled release from chitosan/sodium lauryl ether sulfate microcapsules. *Carbohydrate Polymers*, 251, 116988. <https://doi.org/10.1016/j.carbpol.2020.116988>
- Calderón-Oliver, M., Pedroza-Islas, R., Escalona-Buendía, H. B., Pedraza-Chaverri, J., & Ponce-Alquicira, E. (2017). Comparative study of the microencapsulation by complex coacervation of nisin in combination with an avocado antioxidant extract. *Food Hydrocolloids*, 62, 49-57. <https://doi.org/10.1016/j.foodhyd.2016.07.028>
- Camacho, D. H., Uy, S. J. Y., Cabrera, M. J. F., Lobregas, M. O. S., & Fajardo, T. J. M. C. (2019). Encapsulation of folic acid in copper-alginate hydrogels and its slow in vitro release in physiological pH condition. *Food Research International*, 119, 15-22. <https://doi.org/10.1016/j.foodres.2019.01.053>
- Castelo, R. M., da Silva, L. C., Sousa, J. R., Magalhães, H. C. R., & Furtado, R. F. (2020). Development and Characterization of Pequi Oil (*Caryocar coriaceum* Wittm.) Microparticles by Vibration Nozzle Encapsulation. *Macromolecular Symposia*, 394(1), 2000061. <https://doi.org/10.1002/masy.202000061>
- Celli, G. B., & Brooks, M. S. L. (2017). Impact of extraction and processing conditions on betalains and comparison of properties with anthocyanins — A current review. *Food Research International*, 100(Part 3), 501-509. <https://doi.org/10.1016/j.foodres.2016.08.034>
- Costa, P. J. C. (2002). Avaliação *in vitro* da lioequivalência de formulações farmacêuticas. *Revista Brasileira de Ciências Farmacêuticas*, 38(2), 141-153. <https://doi.org/10.1590/S1516-93322002000200003>
- da Silva Carvalho, A. G., da Costa Machado, M. T., de Freitas Queiroz Barros, H. D., Cazarin, C. B. B., Maróstica Junior, M. R., & Hubinger, M. D. (2019). Anthocyanins from jussara (*Euterpe edulis* Martius) extract carried by calcium alginate beads pre-prepared using ionic gelation. *Powder Technology*, 345, 283-291. <https://doi.org/10.1016/j.powtec.2019.01.016>
- Da Silveira Cáceres de Menezes, M. F., Rodrigues, L. Z., Cavalheiro, C. P., Etchepare, M. A., & Ragagnin de Menezes, C. (2015). Microencapsulação de probióticos por gelificação iônica externa utilizando pectina. *Ciência e Natureza*, 37(5), 30-37. <https://doi.org/10.5902/2179-460X19712>
- Dalponte Dallabona, I., de Lima, G. G., Cestaro, B. I., Tasso, I. de S., Paiva, T. S., Laureanti, E. J. G., Jorge, L. M. de M., da Silva, B. J. G.,

- Helm, C. V., Mathias, A. L., & Jorge, R. M. M. (2020). Development of alginate beads with encapsulated jabuticaba peel and propolis extracts to achieve a new natural colorant antioxidant additive. *International Journal of Biological Macromolecules*, 163, 1421-1432. <https://doi.org/10.1016/j.ijbiomac.2020.07.256>
- Deladino, L., Anbinder, P. S., Navarro, A. S., & Martino, M. N. (2008). Encapsulation of natural antioxidants extracted from *Ilex paraguariensis*. *Carbohydrate Polymers*, 71(1), 126-134. <https://doi.org/10.1016/j.carbpol.2007.05.030>
- Dodero, A., Pianella, L., Vicini, S., Alloisio, M., Ottonelli, M., & Castellano, M. (2019). Alginate-based hydrogels prepared via ionic gelation: An experimental design approach to predict the cross-linking degree. *European Polymer Journal*, 118, 586-594. <https://doi.org/10.1016/j.eurpolymj.2019.06.028>
- Ferreira, M., Pradela Filho, L., Santos, A., Takeuchi, R., & Assunção, R. (2019). Avaliação do perfil de liberação do fármaco ibuprofeno em membranas simétricas e assimétricas de acetato de celulose: efeito da morfologia. *Química Nova*, 42(8), 823-830. <https://doi.org/10.21577/0100-4042.20170409>
- Günter, E. A., Martynov, V. V., Belozerov, V. S., Martinson, E. A., & Litvinets, S. G. (2020). Characterization and swelling properties of composite gel microparticles based on the pectin and  $\kappa$ -carrageenan. *International Journal of Biological Macromolecules*, 164, 2232-2239. <https://doi.org/10.1016/j.ijbiomac.2020.08.024>
- Kouamé, K. J. E. P., Bora, A. F. M., Li, X., Sun, Y., & Liu, L. (2021). Novel trends and opportunities for microencapsulation of flaxseed oil in foods: A review. *Journal of Functional Foods*, 87, 104812. <https://doi.org/10.1016/j.jff.2021.104812>
- Kurozawa, L. E., & Hubinger, M. D. (2017). Hydrophilic food compounds encapsulation by ionic gelation. *Current Opinion in Food Science*, 15, 50-55. <https://doi.org/10.1016/j.cofs.2017.06.004>
- Kurtulbaş, E., Albarri, R., Torun, M., & Şahin, S. (2022). Encapsulation of Moringa oleifera leaf extract in chitosan-coated alginate microbeads produced by ionic gelation. *Food Bioscience*, 50(Part B), 102158. <https://doi.org/10.1016/j.fbio.2022.102158>
- Labus, K., Trusek-Holownia, A., Semba, D., Ostrowska, J., Tynski, P., & Bogusz, J. (2018). Biodegradable polylactide and thermoplastic starch blends as drug release device – mass transfer study. *Polish Journal of Chemical Technology*, 20, 75-80. <https://doi.org/10.2478/pjct-2018-0011>
- Li, L., Zhang, M., Feng, X., Yang, H., Shao, M., Huang, Y., Li, Y., & Teng, F. (2023). Internal/external aqueous-phase gelation treatment of soybean lipophilic protein W/O/W emulsions: Improvement in microstructure, interfacial properties, physicochemical stability, and digestion characteristics. *Food Hydrocolloids*, 136(Part A), 108257. <https://doi.org/10.1016/j.foodhyd.2022.108257>
- Li, L., Zhao, J., Sun, Y., Yu, F., & Ma, J. (2019). Ionically cross-linked sodium alginate/ $\kappa$ -carrageenan double-network gel beads with low-swelling, enhanced mechanical properties, and excellent adsorption performance. *Chemical Engineering Journal*, 372, 1091-1103. <https://doi.org/10.1016/j.cej.2019.05.007>
- Li, X., Zhang, Z. H., Qiao, J., Qu, W., Wang, M. S., Gao, X., Zhang, C., Brennan, C. S., & Qi, X. (2022). Improvement of betalains stability extracted from red dragon fruit peel by ultrasound-assisted microencapsulation with maltodextrin. *Ultrasonics Sonochemistry*, 82, 105897. <https://doi.org/10.1016/j.ultsonch.2021.105897>
- Lin, D., Kelly, A. L., & Miao, S. (2021). Alginate-based emulsion micro-gel particles produced by an external/internal O/W/O emulsion-gelation method: Formation, suspension rheology, digestion, and application to gel-in-gel beads. *Food Hydrocolloids*, 120, 106926. <https://doi.org/10.1016/j.foodhyd.2021.106926>
- Luiza Koop, B., Nascimento da Silva, M., Diniz da Silva, F., Thayres dos Santos Lima, K., Santos Soares, L., José de Andrade, C., Ayala Valencia, G., Rodrigues & Monteiro, A. (2022). Flavonoids, anthocyanins, betalains, curcumin, and carotenoids: Sources, classification and enhanced stabilization by encapsulation and adsorption. *Food Research International*, 153, 110929. <https://doi.org/10.1016/j.foodres.2021.110929>
- Lupo, B., Maestro, A., Gutiérrez, J.M., & González, C. (2015). Characterization of alginate beads with encapsulated cocoa extract to prepare functional food: Comparison of two gelation mechanisms. *Food Hydrocolloids*, 49, 25-34. <https://doi.org/10.1016/j.foodhyd.2015.02.023>
- Naranjo-Durán, A. M., Quintero-Quiroz, J., Rojas-Camargo, J., & Ciro-Gómez, G. L. (2021). Modified-release of encapsulated bioactive compounds from annatto seeds produced by optimized ionic gelation techniques. *Scientific Reports*, 11, 1317. <https://doi.org/10.1038/s41598-020-80119-1>
- Noor, A., Al Murad, M., Jaya Chitra, A., Babu, S. & Govindarajan, S. (2022). Alginate based encapsulation of polyphenols of Piper betel leaves: Development, stability, bio-accessibility and biological activities. *Food Bioscience*, 47, 101715. <https://doi.org/10.1016/j.fbio.2022.101715>
- Otálora, M. C., Carriazo, J. G., Osorio, C., & Nazareno, M. A. (2018). Encapsulation of cactus (*Opuntia megacantha*) betaxanthins by ionic gelation and spray drying: A comparative study. *Food Research International*, 111, 423-430. <https://doi.org/10.1016/j.foodres.2018.05.058>
- Rajmohan, D., & Bellmer, D. (2019). Characterization of Spirulina-Alginate Beads Formed Using Ionic Gelation. *International Journal of Food Science*, 2019, 7101279. <https://doi.org/10.1155%2F2019%2F7101279>
- Riley, N. A. (1941). Projection Sphericity. *Journal of Sedimentary Petrology*, 11(2), 94-95. <https://doi.org/10.1306/D426910C-2B26-11D7-8648000102C1865D>
- Rodríguez-Félix, F., Corte-Tarazón, J. A., Rochín-Wong, S., Fernández-Quiroz, J. D., Garzón-García, A. M., Santos-Sauceda, I., Plascencia-Martínez, D. F., Chan-Chan, L. H., Vásquez-López, C., Barreras-Urbina, C. G., Olguin-Moreno, A., & Tapia-Hernández, J. A. (2022). Physicochemical, structural, mechanical and antioxidant properties of zein films incorporated with no-ultrafiltered and ultrafiltered betalains extract from the beetroot (*Beta vulgaris*) bagasse with potential application as active food packaging. *Journal of Food Engineering*, 334, 111153. <https://doi.org/10.1016/j.jfoodeng.2022.111153>
- Shaddel, R., Hesari, J., Azadmard-Damirchi, S., Hamishehkar, H., Fathi-Achachlouei, B., & Huan, Q. (2018). Use of gelatin and gum Arabic for encapsulation of black raspberry anthocyanins by complex coacervation. *International Journal of Biological Macromolecules*, 107(Part B), 1800-1810. <https://doi.org/10.1016/j.ijbiomac.2017.10.044>
- Silva, L. C., Castelo, R. M., Magalhães, H. C. R., Furtado, R. F., Cheng, H. N., Biswas, A., & Alves, C. R. (2022). Characterization and controlled release of pequi oil microcapsules for yogurt application. *LWT - Food Science and Technology*, 157, 113105. <https://doi.org/10.1016/j.lwt.2022.113105>
- Somacal, S., Somacal, S., Pinto, V. S., de Deus, C., Vendruscolo, R. G., de Almeida, T. M., Wager, R., Mazutti, M. A., & de Menezes, C. R. (2022). Strategy to increase the lipid stability of the microbial oil produced by *Umbelopsis isabellina* for food purposes: Use of microencapsulation by external ionic gelation. *Food Research International*, 152, 110907. <https://doi.org/10.1016/j.foodres.2021.110907>

- Wang, X., Yin, H., Chen, Z., Xia, L. (2020). Epoxy resin/ethyl cellulose microcapsules prepared by solvent evaporation for repairing microcracks: Particle properties and slow-release performance. *Materials Today Communications*, 22, 100854. <https://doi.org/10.1016/j.mtcomm.2019.100854>
- Wang, W., Sun, R., Xia, Q. (2023). Influence of gelation of internal aqueous phase on in vitro controlled release of W1/O/W2 double emulsions-filled alginate hydrogel beads. *Journal of Food Engineering*, 337, 111246. <https://doi.org/10.1016/j.jfoodeng.2022.111246>
- Waqas, M. K., Safdar, S., Buabeid, M., Ashames, A., Akhtar, M., & Murtaza, G. (2022). Alginate-coated chitosan nanoparticles for pH-dependent release of tamoxifen citrate. *Journal of Experimental Nanoscience*, 17(1), 522-534. <https://doi.org/10.1080/17458080.2022.2112919>
- Wongverawattanakul, C., Suklaew, P. on, Chusak, C., Adisakwattana, S., & Thilavech, T. (2022). Encapsulation of Mesona chinensis Benth Extract in Alginate Beads Enhances the Stability and Antioxidant Activity of Polyphenols under Simulated Gastrointestinal Digestion. *Foods*, 11(15), 2378. <https://doi.org/10.3390/foods11152378>
- Xu, J. B., Bartley, J. P., & Johnson, R. A. (2003). Preparation and characterization of alginate-carrageenan hydrogel films cross-linked using a water-soluble carbodiimide (WSC). *Journal of Membrane Science*, 218(1-2), 131-146. [https://doi.org/10.1016/S0376-7388\(03\)00165-0](https://doi.org/10.1016/S0376-7388(03)00165-0)
- Yang, W., Kaimainen, M., Järvenpää, E., Sandell, M., Huopalahti, R., Yang, B., & Laaksonen, O. (2021). Red beet (*Beta vulgaris*) betalains and grape (*Vitis vinifera*) anthocyanins as colorants in white currant juice – Effect of storage on degradation kinetics, color stability and sensory properties. *Food Chemistry*, 348, 128995. <https://doi.org/10.1016/j.foodchem.2020.128995>
- Yousefi, M., Khanniri, E., Shadnoush, M., Khorshidian, N., & Mortazavian, A. M. (2020). Development, characterization and in vitro antioxidant activity of chitosan-coated alginate microcapsules entrapping *Viola odorata* Linn. extract. *International Journal of Biological Macromolecules*, 163, 44-54. <https://doi.org/10.1016/j.ijbiomac.2020.06.250>
- Zanetti, B. G., Soldi, V., & Lemos-Senna, E. (2002). Efeito da adição de polietilenoglicóis nas formulações de microesferas de acetobutirato de celulose sobre a eficiência de encapsulação da carbamazepina e morfologia das partículas. *Revista Brasileira de Ciência do Solo*, 38(2), 229-236. <https://doi.org/10.1590/S1516-93322002000200012>
- Zhang, H., Tan, S., Gan, H., Zhang, H., Xia, N., Jiang, L., Ren, H., & Zhang, X. (2023). Investigation of the formation mechanism and  $\beta$ -carotene encapsulation stability of emulsion gels based on egg yolk granules and sodium alginate. *Food Chemistry*, 400, 134032. <https://doi.org/10.1016/j.foodchem.2022.134032>
- Zhang, R., Zhou, L., Li, J., Oliveira, H., Yang, N., Jin, W., Zhu, Z., Li, S., & He, J. (2020). Microencapsulation of anthocyanins extracted from grape skin by emulsification/internal gelation followed by spray/freeze-drying techniques: Characterization, stability and bioaccessibility. *LWT - Food Science and Technology*, 123, 109097. <https://doi.org/10.1016/j.lwt.2020.109097>
- Zhu, Z., Hu, J., & Zhong, Z. (2022). Preparation and characterization of long-term antibacterial and pH-responsive Polylactic acid/Octenyl succinic anhydride-chitosan @ tea tree oil microcapsules. *International Journal of Biological Macromolecules*, 220, 1318-1328. <https://doi.org/10.1016/j.ijbiomac.2022.09.038>